Bubbles dynamics under pool scrubbing conditions for iodine compounds trapping applications

Mohamad Farhat, Philippe Nerisson, Maxime Chinaud, Olivier Vauquelin, Laurent Cantrel

Bubbles dynamics under pool scrubbing conditions for iodine compounds trapping applications

M. FARHAT[1,2], P. NERISSON[1], M. CHINAUD[2], Olivier VAQUELIN[2], L. CANTREL[1]

[1]: Institut de Radioprotection et de Sûreté Nucléaire (IRSN), 13115 St Paul Lez Durance
[2]: Aix-Marseille Université, IUSTI UMR 7343, 5 rue Enrico Fermi, 13453 Marseille

Mohamad.Farhat@irsn.fr

ABSTRACT

Accident management systems are highly regarded in the designing of nuclear power plants, in order to mitigate as much as possible the radiological consequences of accidents. Wet FCVS is one of these systems that aims to trap fission products in liquid bath by pool scrubbing as well as suppression pool in BWR.
Relying on set of bubble dynamics and retention mechanisms, it is essential to characterize the relevant hydrodynamics in pool scrubbing conditions, for the development and assessment of models. Injecting air induces bubble-bubble interactions which provoke, depending on the flow rate, random formation of bubbles affecting their size, shape, and frequency of bubbling.
Experimental work is carried out to reveal the impact of these interactions on the formation of bubbles at a submerged orifice. Based on the different bubble's morphologies that have been observed, we first investigated the bubble-bubble interactions and then classified different bubbling regimes depending on the position of bubbles' coalescence. The biggest bubble formed above the orifice, after the coalescence of bubbles, is referred by a globule. On the basis of the morphological description of bubbles throughout our experiments, two approaches in characterizing the bubbles sizes were developed. The first conventional approach is based on the assumption of single bubbling formation and spherical shape of bubbles. Upon this approach, the comparison of characteristic bubble size V_b, which is computed after determining the bubble departure frequency f_b, shows a good agreement with literature models. However, this approach is not consistent with flow morphology experimentally observed. Therefore, and through a proposed phenomenological approach, we aimed to characterize experimentally the globule formation frequency f_G and its volume V_G, by tracking the globules formation through image processing and reconstructing bubble shape with axisymmetric assumption. Experimental work characterizing bubble dynamics in the injection zone for different flow conditions (orifice diameter, injection flowrate, and submergence) is presented. In parallel, decontamination factors (DF) for iodine compounds are experimentally determined, in order to be able in the long term to correlate iodine trapping with hydrodynamics considerations.

Keywords: Pool scrubbing, bubble dynamics, aperiodic formation, bubble volume

1. INTRODUCTION

In a severe nuclear accident where a significant damage of reactor fuel results in partial or complete core meltdown, fission products can be transported by various natural processes (chemical reactions, aerosol behaviour, condensation, etc.) into the containment or environment. The PWR (Pressurized Water Reactor) nuclear facilities are therefore featured and equipped with accident management systems designed to prevent potential abnormal situations and limit their hazardous consequence in case of any accident. One of these

systems is the Filtered Containment Venting System, FCVS [1], which aims to prevent containment failure (removing heat and attenuating pressure) by venting its atmosphere comprising fission products into liquid pools [2]. Pool scrubbing can also occur in SGTR (Steam Generator Tube Rupture) accidental situation on PWR and in pressure suppression pools on BWR (Boiling Water Reactor). This bubbling of the gaseous radioactive material leads to the formation of bubbles. During their rise along the pool, fission products can reach the bubble surface due to mass transfer mechanisms, then, are trapped in the liquid pool. This phenomenon, known as pool scrubbing, has the potential to reduce the release of radioactive species to environment. Pool scrubbing relies on set of bubble dynamics and mass transfer mechanisms into the liquid phase, which are dependent of different flow conditions. For that, extensive experimental programs have been conducted to characterize the bubble hydrodynamics and retention of mixtures carried by injected gas into liquid pools [3]. Yet, developed pool scrubbing codes (BUSCA, SUPRA, SPARC) have not shown accurate simulations for the existing experimental databases in determining decontamination factor (DF). The latter refers to retention efficiency as it is the ratio of fission product mass flowrate entering the pool to the fission product mass flow rate leaving it.

$$DF = \frac{\dot{m}_{in}}{\dot{m}_{out}}$$

Large effort is ongoing in the frame of the IPRSECA project to cover this issue.
In order to improve the pool scrubbing and retention modelling, a better characterization of bubble hydrodynamics should be performed, apart from classical assumptions, and considering different encountering phenomena. Since massive research have been conducted to characterize the behavior and dynamics of bubble formation [4-6], however few of them aimed to characterize the chaotic behavior bubbling [7-8]. That is because in high flowrate injection systems, bubble-bubble interactions is considered to be key of nonlinear behavior of bubbles, as inertial effects over dominate the interfacial – viscous forces. In Farhat et al. [9], it is reported that classical approaches to characterize the bubble dynamics are not consistent with the flow morphology. There is a large uncertainty for classical models in predicting the bubbles sizes, therefore, the corresponding mass transfer. Kyriakides [8] et al. stated that beyond a certain flowrate, an irregular large bubble is formed after the coalescence of several bubbles just above the orifice, which is characterized phenomenologically in Farhat et al.

In the pool scrubbing facility there are three hydrodynamic zones in the pool. Each zone has its specific contribution depending on different removal mechanisms. There is an injection zone where there is the globule bubble formation, then the transition zone where globule breaks up during its rising and finally there the bubble rise zone which is identified as a horizontally expanding bubble swarm that consists of tiny equal sized bubbles. Given that significant retention in expected by some authors in the injection zone [10], experimental work is carried out in the present study to characterize the bubble dynamics in this zone.

Thus, in the present study, experimental work is carried out to characterize the bubble dynamics in the injection zone for different flow conditions (orifice diameter, injection flowrate, and submergence). An optical technique was implemented in order to characterize the globule formed from different orifices sizes at different flow rates and pool submergence. Besides, first experiments of DF measurements have been performed simultaneously, for CsI aerosols. Finally, the dependence of the decontamination factor on the injection flow rate and Weber number, $We = \frac{\rho_g {U_{inj}}^2 d_o}{\sigma} = \frac{16\,\rho_g {Q_{inj}}^2}{\sigma\pi^2 {d_o}^3}$, will be discussed.

2. EXPERIMENTAL WORK

Different techniques have been used in the literature for investigation of bubbling through submerged orifice [11-14]. At high flowrates, bubbles behavior limit the capability of techniques that provide local measurements, due to the bubble-bubble interactions. In our experiments, bubble hydrodynamics

measurements are carried out mainly with a high-speed camera technique, and based on images processing, allowing tracking of bubbles evolution. In parallel, DF measurements are performed by determining CsI quantities upstream and downstream the liquid bath, using chemical analysis techniques.

2.1. Experimental setup

The experimental tests were carried out on TYFON (Trapping and hYdrodynamics of FissiON products behaviour in pool scrubbing) facility, shown on figures 1 and 2. The facility is designed to perform experiments coupling hydrodynamic, thermal hydraulic, and decontamination factor measurements for various FP compounds (iodine compounds such as volatile I_2 or CH_3I, aerosols). Eventually, this allows to investigate the dependence of the bubble hydrodynamics and decontamination factor on the different experimental aspects.
Air is injected from single nozzle (2 mm, 5 mm, 10 mm, 20 mm, and 50 mm) submerged in a stagnant liquid column. The bubble column is of 500 mm internal diameter and afford pool submergence of 1.3 m, which corresponds to a volume of 250 L. The interior walls of the column are made up of stainless steel ‘‘mirror polished’’ to effectively prevent the adsorption of iodine composites on its surfaces. Moreover, it is equipped with six transparent windows permitting visualization of flow using the high-speed camera ‘’Phantom Speed sense” VEO-E’’, which could take 3000 images per second at 1280 × 800 pixels.

Figure 1- TYFON facility

The column is thermally insulated, and the liquid bath can be heated up to 90°C according to heating cords around the column external surface. Five thermocouples are distributed between the injection and the height of the free surface of the pool, to maintain the temperature's measurement of the pool.

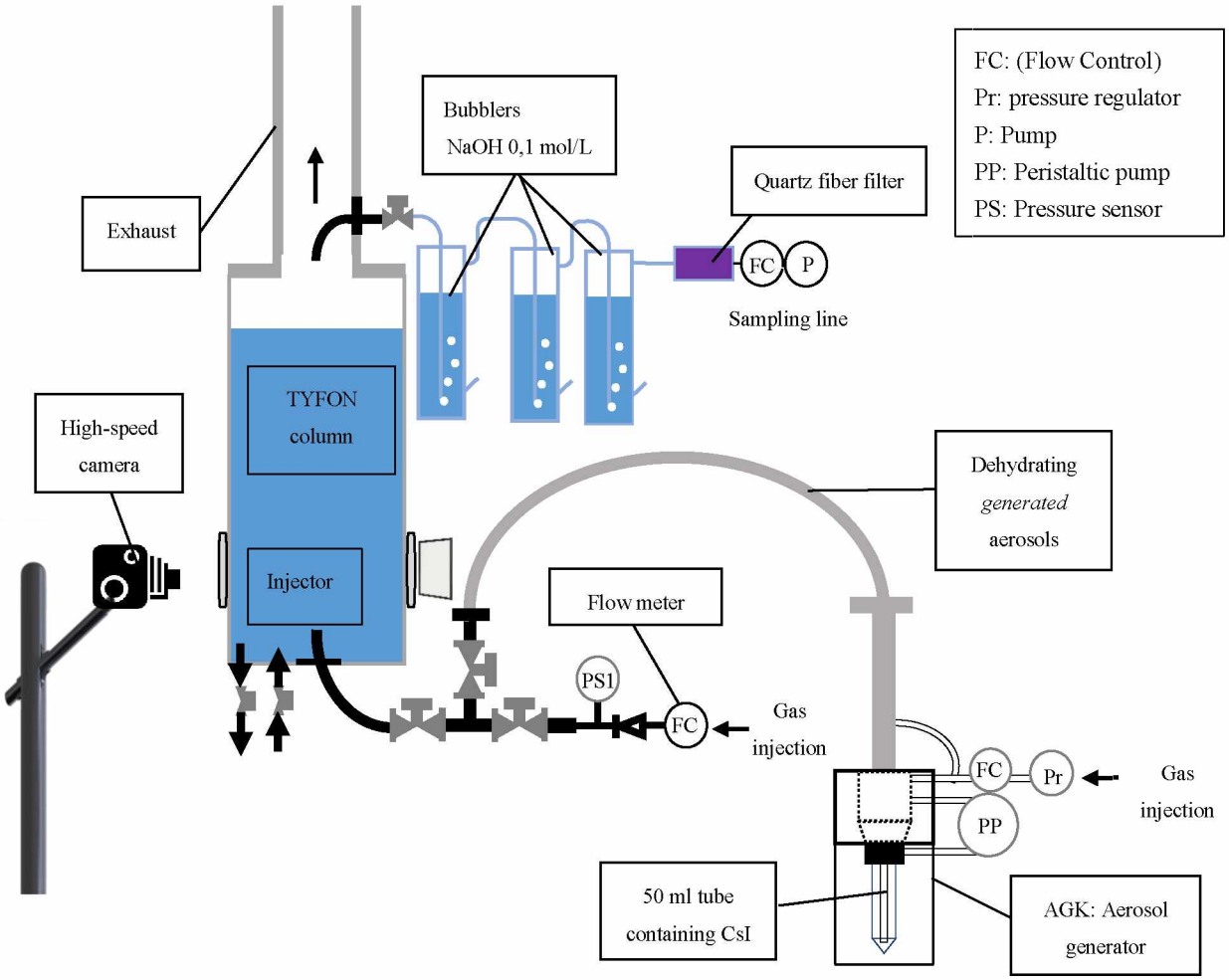

Figure 2- Schema of the experimental setup in CsI injection configuration

2.2. Data treatment

The measurement system of bubble hydrodynamics is composed of a high-speed camera, a LED light source with a diffuser, and associated to the Dantec-Dynamics software. A high-speed camera is used to obtain the flow visualizations and describe the bubble shapes and sizes by image processing. Acquisition of images is performed with 2500 images per second, lasting for 30 seconds.

A background light is used on the opposite window to the camera, in order to compensate the illumination while setting low aperture values of the camera. The latter serves in decreasing the obscurity of images due to the rapid motion of bubbles.

The contrast of the raw images are adjusted and blurred to reduce background noise. This is followed by removing noise from images through filtering the grey-scale images using a pixel-wise adapting low-pass

wiener filter. Thereafter, the contours of structures are detected using the edge-detection algorithm as shown in figure 3.

Figure 3- Image processing; (a): Sobel filter, (b): Binarization, (c): Detection of contours

2.3. Globule characterization

The formation and rising process along the pool exhibit different behavior and regimes. Thanks to the different phenomenology encountered in each zone, it is possible to distinguish the onset of each zone. There is an injection zone where there is the globule formation, which is the biggest bubble formed above the orifice, after the coalescence of bubbles. Then the bubbles break up during the rising flow (break up zone) and finally there is a zone with the bubble swarm (bubble rise zone, where bubbles reach their terminal velocities).

2.3.1 Globule frequency

For the frequency of globule, an event is recorded when a complete formation of a globule is achieved. The latter takes in consideration the coalescences of two or more or bubbles and the re-attachment of the formed structure to the orifice. The quantification of the globules formation is done through analyzing a chronograph of bubbles evolution. Therefore, we are capable of differentiating between the events of bubbles departure and globule formation [9].

2.3.2. Globule Volumes

At the instant where a detected structure is detached finally from the orifice, the globule volume is computed numerically by considering a unitary volume corresponding to a pixel in a binarized image. Then a cylindrical revolution of the pixels is assumed around an equidistant line with ax-symmetric assumption.

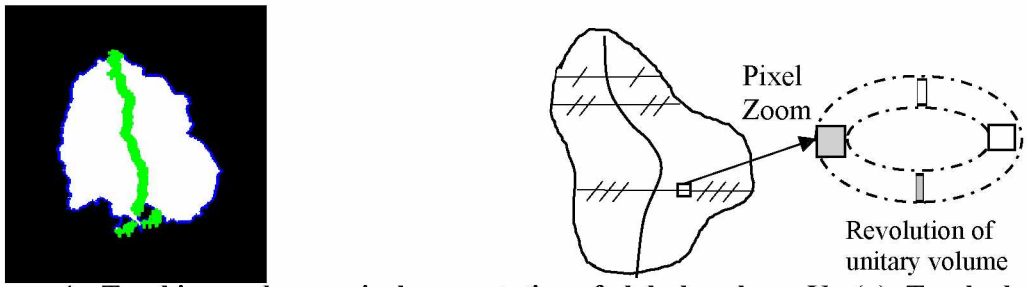

Figure 4-: Tracking and numerical computation of globule volume $V_{G;}$ (a): Tracked globule, (b): Schema of unitary volume of a pixel

Thus, the volume of revolution (1-pixel torus) is computed for each pixel (rotation, see figure 4). Therefore, the volume of each cylindrical slice of the structure is the sum of all 1-pixel torus volumes of the corresponding slice. Finally, the volume of the structure is the sum of all cylinder volumes calculated along the equidistant line. This phenomenological approach is validated by comparing Q_{exp} (V_G, f_G) to the real injected flowrate Q_{real}, which are consistent [9] (see results below).

2.4. DF measurements

Cesium iodide aerosols were injected into the TYFON facility, using Palas AGK 2000 generator. The median mass aerodynamic diameter (MMAD) for CsI aerosols is 1 µm (dispersion $\sigma_g = 1.8$). The mean aerosol flow rate is between 0.2 and 0.4 $mg.min^{-1}$.A sampling system (shown in figure 2) is used downstream the bath to measure outlet CsI concentration.

The amount of CsI aerosols injected is the sum of the amount of CsI trapped in the pool with the amount of CsI transferred through the pool, which is measured in the sampling system. Taking in consideration the aerosol deposition on the surfaces, notably in the sampling system (isokinetic cane, pipes) in addition to the deposition on the quartz filter, sample washing is done to collect all the deposited quantity of CsI aerosols. All the liquid samples are then analyzed by inductively coupled plasma - mass spectrometry ICP-MS.

3. RESULTS AND DISCUSSION

In pool scrubbing scenarios, tests parameters may favor or hinder the retention of fission products. It is therefore important to investigate the influence of these parameters on the bubble dynamics in order to correlate with decontamination factor measurements. In the following paragraphs, the possible impacts of contamination, injection flow rate, orifice size, and pool submergence, are characterized on the globule formation in the injection zone. At this stage, all the presented results have been obtained at ambient temperature for gas and liquid bath.

3.1. Effect of contamination

In our test conditions, it was experimentally checked that there is no significant change in the globule volume when feeding the carrier gas by these CsI particles, as shown in the figure 5.

This may be due to the low concentration of aerosols depositing on the globules, this is consolidated by the ratio in size of the aerosol's particles to globule volume [15]: for We = 0,077, this ratio is around $4.4x10^{-3}$.

3.2. Variation of test conditions

Five orifices were used to compare their influence on the globule size. For the 50 mm orifice, no globule formation was observed. Instead, a swarm of smaller bubbles was formed within the tips of the orifices. This can be due to the weak effect of surface tension (orifice – air – water) in front of the inertial and gravitational forces. For the other orifices (2 mm, 5 mm, 10 mm, 20mm), globule formation was characterized for different injection flowrates and pool submergence.

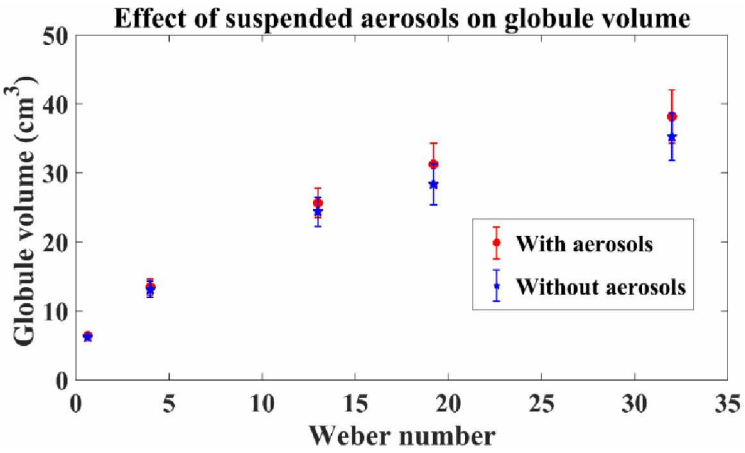

Figure 5- Effect of aerosol suspension on globule volume at ambient temperature

3.2.1- Effect of orifice size

In the figure 6, the globule volume is presented as function of Weber number that varies due to both the orifice size and injection flow rate. A significant increase in globule volume is shown with higher orifice size for same Weber number.

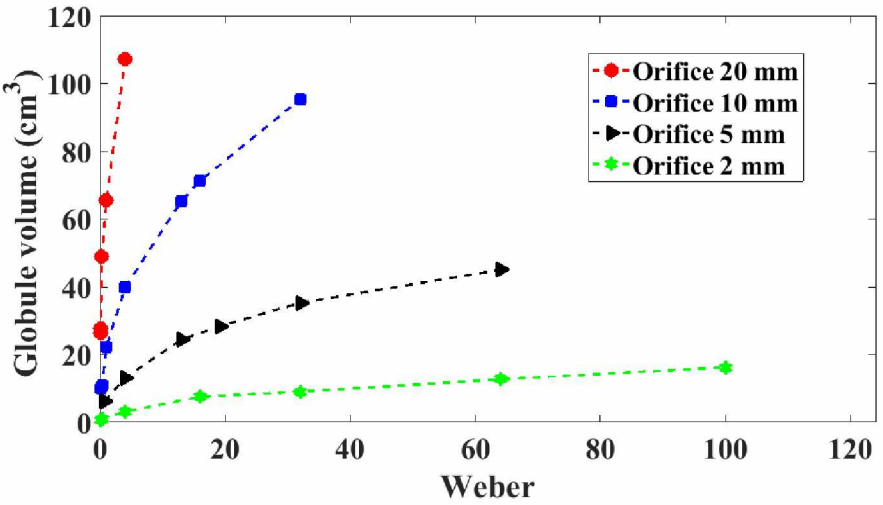

Figure 6- Variation of globule volume for different orifices

Owing to the strong dependence of Weber number on the orifice size, and in order to differentiate between the contribution of orifice size and injection flow rate, the impact of gas flow rate for different orifices is presented in figure 7.

Despite the size of orifice, comparable values of globule volumes for same flow rate are maintained. For orifice of 20 mm, there is slight increase which is due to the higher formation time needed in order to form bubbles between the tips of the orifice, as shown in figure 7. Figure 8 illustrates and consolidates this statement, where the globule frequency of 20 mm orifice is smaller than other globule frequencies of different orifices sizes.

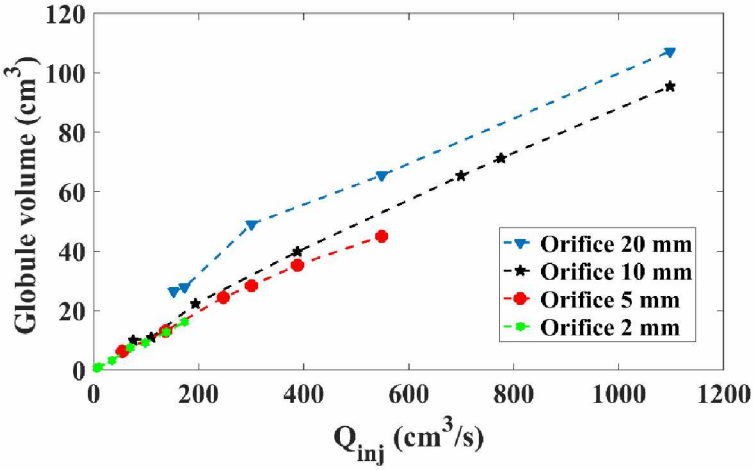

Figure 7- Variation of gluble volume as function of injection flowrate

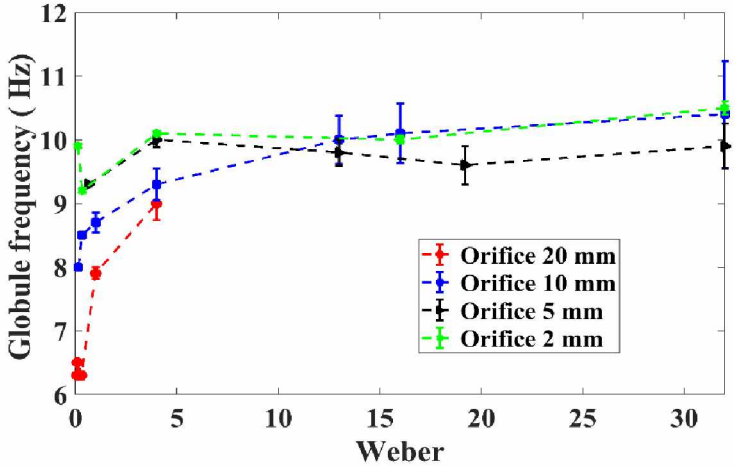

Figure 8- Globule frequency for different orifices at ambient temperature

Moreover, we assume that $Q_{calc} = V_G \times f_G$, where V_G and f_G are respectively the volume and frequency of the globules. This assumption stems from the fact the formation of globule is common and relevant along the different flow morphologies. Therefore, as explained in [9] to validate the method (cf. section 2.3.2), the injection flowrate Q_{real} must be correlated to the volume of globule V_G formed at frequency f_G. Figure 9 shows that the experimental data fits reasonably the actual injection flowrate for the different orifices.

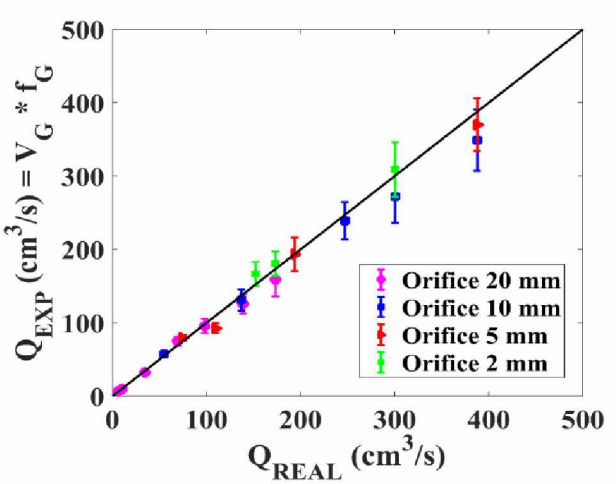

Figure 9- Validation of experimental flowrate with actual flowrate

3.2.2 Effect of pool submergence

According to Kumar and Kuloor [16], above a certain altitude of the pool surface, volume of bubbles forming at a submerged orifice for a constant air flow rate are not affected. Nevertheless, it may affect the bubble volume appreciably in the intermediate region.

The pool submergence was set to 5 different altitudes according to Y_{max} which refers to the altitude of the injection zone (i.e.: the onset of breakup zone where the globule starts fragmentation).

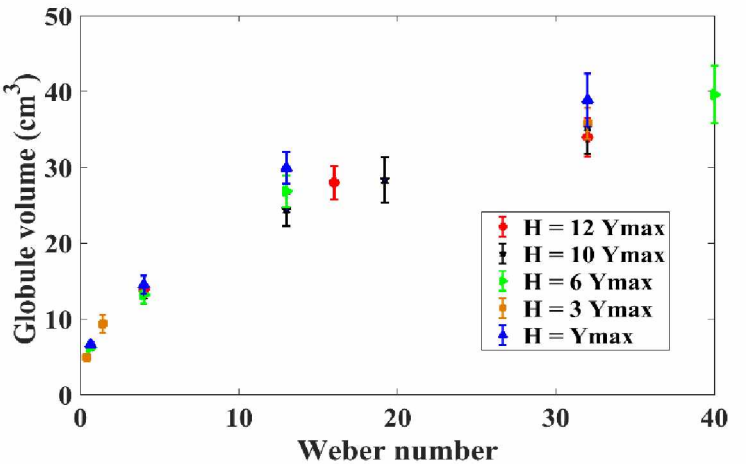

Figure 10- Globule volume for different pool submergences at ambient temperature

For a given We, no significant variation was found on the volume of globule except at the lowest submergence where H = Y_{max}, as shown in figure 10. At this altitude, the globule undergoes a bit larger expansion due to less hydrostatic pressure on the interface of the bubble. However, and despite the variation hydrostatic pressure, the inertial effects over dominate the latter mechanism

3.3. Effect of Weber Number on Decontamination Factor

First tests were carried out to investigate mainly the dependence of DF on gas flowrate, consequently Weber number. The parameters of the test are shown in table 1.

Table 1- Tests conditions of DF measurements

Test	We	Air temperature (°C)	Water temperature (°C)	Orifice size (mm)	Pool Submergence (m)
1	0.08	25	25	20	1
2	4.9	25	25	5	1
3	32	25	25	5	1
4	205	25	25	5	1
5	350	25	25	5	1

Zhao et al. [17] considered a critical Weber number $We_{critical}$ for transition from bubbling to jetting regime. This critical Weber number was given by: $We_{critical} = 10.5 \left(\rho_l/\rho_g\right)^{0.5}$ such that $We_{critical} = 316$. According to this criterion, it is considered that different bubbling regimes were examined.
The impact of gas injection flowrate on the retention of aerosols varies between bubbling and jetting regimes. In fact, this parameter prompts counter effect removal mechanisms (gravitational settling, gas residence time, jet impaction, centrifugal impaction).
At very low Weber number, the decontamination factor was found to be relatively high due to high residence time. Moreover, low bubble rising velocities prompts gravitational settling of aerosols. As Weber number increases, DF starts to decrease significantly due to the attenuation of the latter mechanisms. In the regime where it can be described as transition regime ($100 < We < 300$), DF tends to have a similar value. However, as Weber number increases beyond the transition regime, DF tends to increase when the flow is described as jetting regime ($We = 350$). In our test conditions, DF is lower than ~50.
In the latter regime, two main removal mechanisms are present: inertial impaction (deposition velocity of impaction proportional to injection velocity) and surface exchange. When gas flow rate increases in jetting regimes, smaller bubbles in the bubble rise zone are obtained due to a stronger inertial breakup [18], thus provoking higher interfacial area and generally lower terminal velocities[1] [19], inducing higher residence time of bubbles in the bath.

4. CONCLUSIONS

Flow structure in pool scrubbing conditions, where for example air is injected at high momentum, exhibits different patterns than in conventional experiments. That recalls for approaches that could better describe the bubble hydrodynamics due to the different encountered phenomena. Within this concept and its relevance in nuclear safety, experimental work is carried out, in a first step at ambient temperature, to characterize the bubble hydrodynamics in the injection zone. Air is injected from submerged orifices of different sizes, at different flowrates, and through pools of water of different altitudes.
The presence of CsI aerosols has no influence on the globule dynamics, where the respectively large globule volumes can afford the deposition without interfering their surface tension.
Comparable globule volumes and frequencies were reported for the small orifices (2, 5, and 10 mm), where globule volume increases with the injection flowrate. For the large orifice (20 mm), the increase formation time results in a larger globule volume and smaller globule frequency. The phenomenological approach

[1] On the graph plotting terminal velocity vs bubble size, even if the overall curve shape is increasing, a local maximum can be observed for bubble diameter around 1 mm [19].

implemented to determine the globule volume is validated by comparing Q_{calc} (V_G, f_G) to the real injected flowrate Q_{inj}.
Regarding the pool submergence, negligible influence on globule volume was reported where experiments were carried at constant flow and pressure conditions. The dominant mechanisms in the injection zone near the orifice attenuates the effect of hydrostatic pressure induced by the pool submergence.
In fact, while an increase in gas flowrate favors the inertial and centrifugal impaction, it hinders the residence time and gravitational settling. Apparently, in bubbling regimes, the latter mechanisms dominate over the mechanisms induced by the increase of gas flowrate (i.e., inertial and centrifugal impaction, large surface exchange), whereas these phenomena dominate over the residence time once jetting regime reached. In other words, for a given test conditions, the DF variation as a function of We should tend to have a minimum. Beyond this minimum, residence time and gravitational settling effects dominate and above it, effects linked to jetting regime listed above dominate.
Later on, tests will be performed to evaluate the influence of liquid pH and temperatures of bath and/or gas on DF. Besides, DF will be measured for volatile iodine species (I_2, CH_3I).

ACKNOWLEDGMENTS

This work was performed in the French Institut de Radioprotection et de Sûreté Nucléaire (IRSN), with the financial support of French Région Sud- Provence-Alpes-Côte d'Azur and Electricité de France (EDF).

Nomenclature

d_0	Orifice diameter	[m]
Q_{inj}	Injected air volume flow rate	[$m^3.s^{-1}$]
Q_{calc}	Calculated volume flow rate	[$m^3.s^{-1}$]
V_G	Globule volume	[m^3]
U_{inj}	Gas injection velocity	[$m.s^{-1}$]
We	Orifice Weber number:	[-]
$We_{critical}$	Critical Weber number	[-]
Ymax	Height of injection zone	[m]
Greek symbols		
ρ_g	Gas density	[$kg.m^{-3}$]
ρ_l	Liquid density	[$kg.m^{-3}$]
σ	Surface tension	[$N.m^{-1}$]

REFERENCES

1. D. Jacquemain, S. Guentay, S. Basu, M. Sonnenkalb, L. Lebel, J. Ball, H. Allelein, M. Liebana, B. Eckardt, N. Losch, et al., "Oecd/nea/csni status report on filtered containment venting," tech. rep., Organisation for Economic Co-Operation and Development, 2014.
2. Sehgal, Bal Raj, ed. *Nuclear safety in light water reactors: severe accident phenomenology*, Academic Press, 2011.
3. Swiderska-Kowalczyk, M., Escudero-Berzal, M., Marcos-Crespo, M., Martin-Espigares, M., & Lopez-Jimenez, J. *State-of-the-art review on fission product aerosol pool scrubbing under severe accident conditions*, 1996.
4. J. Davidson and B. Schuler, "Bubble formation at an orifice in a viscous liquid," *Transactions of the Institution of Chemical Engineers*, **vol. 38**, pp. 144–154, 1960.
5. E. Gaddis and A. Vogelpohl, "Bubble formation in quiescent liquids under constant flow conditions," *Chemical Engineering Science*, **vol. 41**, no. 1, pp. 97–105, 1986.

6. M. Jamialahmadi, M. Zehtaban, H. Müller-Steinhagen, A. Sarrafi, and J. Smith, "Study of bubble formation under constant flow conditions," *Chemical Engineering Research and Design*, **vol. 79**, no. 5, pp. 523–532, 2001.
7. R. Mosdorf and T. Wyszkowski, "Experimental investigations of deterministic chaos appearance in bubbling flow," *International journal of heat and mass transfer*, **vol. 54**, no. 23-24, pp. 5060–5069, 2011.
8. N. Kyriakides, E. Kastrinakis, S. Nychas, and A. Goulas, "Bubbling from nozzles submerged in water: transitions between bubbling regimes," *The Canadian journal of chemical engineering*, **vol. 75**, no. 4, pp. 684–691, 1997.
9. Farhat, M., Chinaud, M., Nerisson, P. and Vauquelin, O., 2021. Characterization of bubbles dynamics in aperiodic formation. *International Journal of Heat and Mass Transfer*, **vol. 180**, p.121646.
10. Lee, Yoonhee, Yong Jin Cho, and Inchul Ryu. "Preliminary analyses on decontamination factors during pool scrubbing with bubble size distributions obtained from EPRI experiments." *Nuclear Engineering and Technology* 53.2 (2021): 509-521.
11. Q. Cai, X. Shen, C. Shen, and G. Dai, "A simple method for identifying bubbling/jetting regimes transition from large, submerged orifices using electrical capacitance tomography (ect)," *The Canadian Journal of Chemical Engineering*, **vol. 88**, no. 3, pp. 340–349, 2010.
12. J. Cieslinski and R. Mosdorf, "Gas bubble dynamics—experiment and fractal analysis," *International Journal of Heat and Mass Transfer*, **vol. 48**, no. 9, pp. 1808–1818, 2005.
13. V. Badam, V. Buwa, and F. Durst, "Experimental investigations of regimes of bubble formation on submerged orifices under constant flow condition," *The Canadian Journal of Chemical Engineering*, **vol. 85**, no. 3, pp. 257–267, 2007.
14. Y. Abe, K. Fujiwara, S. Saito, T. Yuasa, and A. Kaneko, "Bubble dynamics with aerosol during pool scrubbing," *Nuclear Engineering and Design*, **vol. 337**, pp. 96–107, 2018.
15. Hinds, William C. *Aerosol technology: properties, behavior, and measurement of airborne particles*. John Wiley & Sons, 1999.
16. R. Kumar and N. Kuloor, "The formation of bubbles and drops," *Advances in chemical engineering*, **vol. 8**, pp. 255–368, 1970.
17. Y.-F. Zhao and G. A. Irons, "The breakup of bubbles into jets during submerged gas injection," *Metallurgical Transactions B*, **vol. 21**, no. 6, pp. 997–1003, 1990.
18. A.T. Wassel, A.F.Mills, D.C. Bugby and R.N. Oehlberg. "Analysis of radionuclide retention in water pools", *Nuclear engineering and design*, ***90*(1)**, pp.87-104, 1985.
19. R. Clift, J.R. Grace and M.E. Weber. *Bubbles, drops and particles.* Chapter 7, Academic Press, New York – San Francisco - London, 1978